Journal of Polymer Research (2023) 30:119
https://doi.org/10.1007/s10965-023-03499-8

ORIGINAL PAPER

Effect of poly (acrylamide-co-acrylic acid salt) on anti-aging properties and adhesion between acrylonitrile butadiene rubber and polyester fabric

Ahmed Abdel-Hakim[1] · Abd El-Aziz Arafa El-Wakil[1] · Sawsan Halim[1]

Received: 12 December 2022 / Accepted: 17 February 2023 / Published online: 25 February 2023

Abstract
In this study, a multifunction polymeric adhesion promoter and anti-aging compound based on the triethanolamine salt of acrylamide acrylic acid copolymer (COS) was prepared and characterized using Fourier-transform infrared spectroscopy (FTIR). The impact of different COS contents on the tensile, adhesion, and thermal properties of NBR composite and NBR/PET sandwich was evaluated. The NBR composites containing COS displayed good retention of their mechanical properties with increasing thermal ageing time, while the composite without COS showed a decrease in its mechanical properties. The highest tensile strength (17.5 MPa with a retention value of 0.6%) after 7 days of thermal aging was recorded for NBR composite, which contains 5 phr (parts per hundred parts of rubber) of COS (COS 5), compared to NBR composite without COS (COS 0), which recorded 15.1 MPa with a retention value of -27.4%. In addition, the COS 5 composite displayed an improvement in peel strength of 16.4% compared to the COS 0. The results of the thermogarvemetric analysis (TGA) supported the anti-thermal ageing effect of COS, where the initial decomposition temperature (Ti) value increased by 11.7 and 9.3 °C, after addition of 5 and 10 phr of COS to NBR composite, respectively. In addition, the other thermogravemetric parameters investigated displayed a significant increase in their values, which confirms the improvement in thermal stability of NBR composite in the presence of COS. Also, the air permeability of the PET/NBR sandwich decreased by 80% after the addition of 7.5 phr of COS.

Keywords Adhesion · Mechanical properties · Thermal properties · Air permeability

Introduction

Rubberized fabric can be created by coating textile fabric with impregnation, surface coating, or lamination. The most popular method of surface coating is the spreading of a viscous fluid made of rubber mix (dough) [1]. The improvement of adhesion between fabric or fibers and polymer matrix is usually achieved through physical or chemical modification of the fabric surface or the addition of adhesion promoters [2]. Several efforts have been made to enhance the adhesion between textile fabric and rubber. Doganci [3] investigated the influence of glycidyl polyhedral oligomeric silsesquioxane (GPOSS) on the adhesion properties between PET cord and rubber(natural rubber styrene butadiene rubber blend). It was found that, the tensile strength wasn't significantly changed while the adhesion strength was improved with the highest adhesion strength obtained at 1% of GPOSS. Zhang et al. [4] improved the adhesion of poly(m-aramide) fabric to fluorosilicone rubber using a combination of silane coupling agent and N_2 plasma surface treatment. The silane compound acted as a bonding agent between fabric, and rubber via grafting reaction on both surfaces. Subramanian and Nando [5] used the dry bonding system, which includes resorcinol, silica, and hexamethylenetetramine to improve the adhesion between polychloroprene rubber and polyvinyl alcohol cords and woven fabric. The change in amount of each component had a significant effect on the adhesion between rubber and cords or fabrics. Acrylonitrile butadiene rubber (NBR) belongs to the unsaturated rubber family. NBR is produced from the copolymerization of acrylonitrile and butadiene monomers. NBR has wide applications in the automotive industry, such as oil and fuel resistance seals, tanks, hoses, grommets, etc. As the acrylonitrile content increases, the fuel and oil resistance of NBR increases [6].

✉ Ahmed Abdel-Hakim
ahmedag83@yahoo.com

[1] Materials Testing and Surface Chemical Analysis Laboratory, National Institute of Standards, Tersa Street, El-Harm, Giza, Egypt

PET fabric, a component of the composites under investigation, has poor compatibility due to its inert surface chemical structure and need to further surface modification or the addition of an adhesion promoter to improve its adhesion with different polymeric compounds [7]. Polyethylene terephthalate (PET) was used as a reinforcing agent for natural rubber [8] and styrene butadiene rubber [9] where it exhibited poor adhesion with them in the absence of adhesion promoter or further modifications. The adhesion between NBR and polar fabrics, including PET, is weak [2, 7, 10, 11]. Many efforts have been made to improve the adhesion of NBR to PET fibre or fabric based on the chemical reaction with NBR's -C = C- [2]. Jincheng et al. [7] investigated the effect of two different adhesion promoting systems to improve the adhesion between NBR and PET cords. Where the hydrated silica-resorcinol-hexamethoxymethyl-melamin (HRH) treated system showed more improvement in adhesion between NBR and PET cords than the resorcinol–formaldehyde-latex (RFL) treated system. Razavizadeh and Jamshidi [2] improved the adhesion between NBR and PET fibers via carboxylation of PET fabric surface using ultra violet (UV) irradiation. It was found that the improvement in bonding between NBR and PET is due to the formation of covalent bonds at the rubber/ fabric interface. Han et al. [12] used titanate to improve the adhesion properties between silicone rubber and polyester fabric. The hardness and tensile strength of the silicone rubber composite decreased gradually as the titanate content increased, whereas the peel force increased up to a titanate concentration of 0.2%.

The presence of unsaturation within the rubber matrix causes instability and subsequent degradation when subjected to thermal or oxidative aging which leads to cleavage of rubber chains and thr formation of oxygen containing groups or additional crosslinks within the rubber matrix [13].This degradation will cause a dramatic drop in the physical, chemical, and mechanical properties of rubber composite which is negatively reflected on its service life [14, 15]. To delay the unsaturated rubber degradation process, chemical antioxidants, such as amide compounds are incorporated to enhance the thermal stability of the rubber [16]. As we mentioned above, NBR is one member of the unsaturated rubber family, and thus, an anti-aging agent should be added to its formulas to retard the degradation process and increase the service life.

Jovanović et al. [17] studied the influence of different anti-aging agents on NBR /iron oxide/zinc dimethacrylate composites and found that all anti-aging agents had negative effect on the crosslink density and the mechanical properties of the NBR composite. The best protective effect at 100 °C was provided by diaryl-p-phenylene diamine (DAPD) where the best antioxidant at 120 °C was diphenylamine (DPA). Zhong et al. [18] modified the graphene oxide (GO) by anti-aging agent p-phenylenediamine (PPD) and used it to improve the themal stability of NBR. The results showed that, the thermo-oxidative stability of rubber matrix increased obviously after introducing GO–PPD. The small antiaging compounds can be lost through diffusion to the surface of the composite, followed by evaporation or dissolution in an appropriate solvent. To avoid the loss of antiaging molecules, macromolecular or polymeric antiaging molecules were used [19].

In this study, a multifunction polymeric adhesion promoter and anti-aging compound based on the triethanolamine salt of acrylamide acrylic acid copolymer (COS) was prepared and characterized using Fourier-transform infrared spectroscopy (FTIR). The effect of COS on the adhesion between NBR and PET fabric and the tensile properties of NBR composite were investigated. In addition, COS was used to improve the thermo-oxidative stability of NBR composite. The effect of thermal aging on the tensile of NBR composite and adhesion properties of PET/NBR sandwich which contain different contents of COS, was evaluated. Also, thermogravimetric analysis (TGA) and air permeability were investigated.

Experimental

Materials

Acrylonitrile butadiene rubber (NBR) under trade name KRYNAC® 2850 F was purchased from, Zeon Advanced Polymix, Thailand, where the acrylonitrile content is 27.5 wt.%, density of 0.97 g/cm^3 and Mooney viscosity ML (1 + 4) 100 °C 48. Acrylamide (AAm), acrylic acid (AA) monomers with purity 99%, ammonium persulfate (APS), 98% and triethanolamine (TEA), 98% were obtained from Merck company, Germany. The polyester fabric was obtained from Misr Helwan for textile, Egypt. Carbon black (N220) with External surface area (STSA), m^2/g 106 m^2/g was provided by Alexandria Carbon Black, Egypt. Hexamethylenetetramine (HMT) with purity 99% was purchased from Alfa Aesar, Germany. Other chemicals were provided by El-Gomhouria For Trading Chemicals, Egypt.

Preparation of COS

In a 500 mL three-necked flask with a condenser, glass thermometer, and a N2 gas input, COS was prepared. The flask was filled with 90 g of distilled water and set to a temperature of 90 °C. The stirring rate was adjusted at 250 rpm. 30 g of AAm were dissolved in 30 g distilled water, and mixed with 30 g of AA. The initiator solution was prepared by dissolving 1.2 g APS in 18.8 g distilled water, which was added simultaneously over 3 h with monomer solution after purging by nitrogen gas to remove dissolved oxygen.

To achieve full monomer conversion, the flask contents were maintained at 90 °C for two hours. After cooling to ambient temperature, the flask contents were completely neutralized by triethanolamine up to pH 7. The product was dried at 105 °C for 24 h to remove all water, yielding a high viscosity material. The structure of the COS was confirmed using Fourier-transform infrared spectroscopy (FTIR) Nicolet 380 spectrophotometer, Thermo Scientific, Waltham USA.

Rubber mixing and fabric-rubber sandwich preparation

On a laboratory two roll mill (152 mm-330 mm) with a friction ratio of 1:1.4, the NBR and other ingredients are blended at room temperature. Prior to adding the filler and other components listed in Table 1, the NBR was masticated for 10 min. The carbon black was added within 4 min while the other ingredients were added almost within 5 min. The total mix, after the complete addition of all ingredients, underwent further mastication for 3 min. The different rheometric parameters namely, curing time (t90), scorch time (ts2), minimum torque (ML), and maximum torque(MH), were determined using the Rheometer MDR 2000, Alpha Technologies, UK. The delta torque (ΔM) was calculated by subtracting the ML from MH. The dough was prepared by immersing of small pieces of each mix in toluene (the ratio was 1 part rubber mix: 1.5 parts toluene and then allowing it to swell for 72 h. The swollen rubber was stirred manually every 24 h. The fabric rubber sandwich of thickness 0.7 ± 0.1 mm was obtained by spreading a layer of dough on the fabric using a film applicator. The rubber-coated fabric was folded to form a fabric-rubber sandwich, then rolled around metal drum, and covered with cotton clothes to prevent warping during vulcanization process. The curing process occurred in an air circulating oven set to 155 °C. The vulcanized sheets were prepared by compression molding in an electrically heated press at 155 °C under a pressure of 150 kg/cm^2.

Table 1 Formulations of different mixes[a]

Sample Code	COS 0	COS 2.5	COS 5	COS 7.5	COS 10
NBR	100				
Carbon Black (N550)	25				
Zinc Oxide	5				
Stearic	2				
CBS	1.2				
MBT	0.8				
HMTA	5				
Resorcinol	5				
Hi-Silica	5				
Sulfur					
COS	0	2.5	5	7.5	10

[a]The values of all ingredients are in phr

Mechanical measurements

The tensile properties were measured according to ASTM D412-16. Five dumb-bell shaped samples of each sample were measured using universal tensile testing machine (Zwick Z010, Germany) at crosshead speed of 500 mm/min. The adhesion strength was measured as per ASTM D 413–17 at crosshead speed 50 mm/min using the universal tensile testing machine. Five plane strips having width, length and thickness of $25+3,-0$ mm, 12 ± 0.5 cm and 0.7 ± 0.1 mm, respectively. The parts of one end of the samples were separated by hand to sufficient distance to permit attachment of the separated ends to the grips of the tensile testing machine. The separation of sample layers was done at an angle of approximately 180°.

The thermal aging was performed, according to ASTM D573-19, in an oven at temperature of 70 °C for 7 days. At different times of aging (1, 3 and 7 days) five samples was taken and tested. The retention in the property can be calculated as follows:

$$Retention\ (\%) = 100 \times \frac{(Pa - Pb)}{Pb} \quad (1)$$

where Pa and Pb are the property measured after and before aging, respectively.

Thermogravimetric Analysis (TGA)

The effect of COS on the thermal stability of NBR composite was performed with TGA-60 Shimadzu Company, Japan. 5 mg of all samples were heated from ambient temperature to 600 °C at a rate of 10 °C/min under N2 gas with flow rate 30 ml/min.

Air permeability measurements

The air permeability through the coated fabric of dimension 50*50*0.7 mm was measured using Electronic Air Permeability Tester (SDL 021A). The air permeability values were expressed in cm^3/s/cm^2. The test was conducted at pressure of 999 Pa. Air permeability measurement was carried out according ASTM D737. The results reported here are the average of five measurements for each sample.

Results and discussion

Characterization of poly (AAc-co-AAm)/TEA (COS)

It is well understood that polyacrylic (PAA) has carboxylic acid groups, which could develop different intermolecular interactions like electrostatic interactions, hydrogen bonds, and dipole-ion

interactions with other polymers and surfactants. Many investigations have shown that there are strong interactions of PAA with other polymers and surfactants in aqueous solutions. There is a great potential for utilizing these interactions in different polymeric industrial applications. Intermolecular interactions affect the vibration of groups on polymer segments, this information can be obtained by FTIR analysis. Figure 1 shows the FTIR spectra of poly (AA-co-AAm) and poly (AA-co-AAm)/TEA (COS). The FTIR spectrum of poly (AA-co-AAm) confirms the formation of co-polymer of acrylic acid and acrylamide as are evident from bands that appeared at 3160 and 3310 cm^{-1} which indicates the N–H stretching of acrylamide unit and O–H stretching of acrylate unit respectively. Asymmetrical and symmetrical stretching of C–H are found at 2980 and 2820 cm^{1}, respectively. Carbonyl stretching vibration gives a peaks at 1660 and 1690 cm^{-1}, and no characteristic stretch vibration peak of C=C is found [20]. The reaction of TEA with poly (AA-co-AAm) is confirmed in FTIR spectrum of COS, whereas band that appeared at 3410 cm^{-1} indicates the O–H stretching. Asymmetrical and symmetrical stretching of C–H are found at 2980 and 2820 cm^{1}, respectively. The characteristic peaks of C=O stretching appear at 1590 and 1690 cm^{-1}. Symmetric and asymmetric stretching of COO^{-} are found at 1380 cm1 and 1410 cm^{-1}, respectively in poly(AA-co-AAm) spectrum and at 1360 and 1420 cm-1 in COS spectrum. These results indicate that the carboxylic groups of PAA form hydrogen bonds with NH_2 in acrylamide unit of the copolymer and it dissociated into COO^{-}, which complexes with the TEA [21, 22].

Rheometric properties and crosslink density

Table 2 shows the effect of different COS contents on the rheometric properties of NBR composites. It can be clearly seen that, the difference between minimum torque (ML) and maximum torque (MH), which is expressed by ΔM, decreased gradually with the increase of COS within the NBR composite. This indicates that the stiffness of the rubber composite decreased as the COS content increased. The value of ΔM depends directly on the crosslinking reaction, where the ΔM value increases with the increase in crosslink density [23]. The decrease of ΔM with the increase of COS concentration within the composite is attributed to the crosslink density of the composite decreased gradually with the increase of COS content, where it decreased from 71.89*10 $^{-5}$ g^{-1}.mol for COS0 to 57.47*10 $^{-5}$ g^{-1}.mol for COS10, as indicated in Table 3 [24]. In addition, Table 2 displayed that, the addition of COS to NBR composite accelerated the vulcanization process as indicated by the decreasing of scorch time (ts2), optimum curing time (t90) and cure rate index [CRI = 100/(t90-ts2)]. Nakason et al. [25] found that the addition of fillers that contain hydroxyl groups in their structure to the rubber composite can accelerate the vulcanization process. In our case, we had a similar result, where the acceleration action of COS can be attributed to the presence of many hydroxyl groups in its structure. Table 3 displayed that, the crosslink density of the NBR

Table 2 Rheometric properties of the different formulations

Sample Code	COS 0	COS 2.5	COS 5	COS 7.5	COS 10
ML (kg-cm)	0.33	0.4	0.56	0.59	0.37
MH (kg-cm)	15.1	14.8	14.4	13.85	13.54
ΔM	14.77	14.4	13.84	13.26	13.17
ts2	0.52	0.48	0.42	0.4	0.39
t90	3.05	3.11	3.08	3.37	3.43
CRI	39.53	38.02	37.59	33.67	32.89

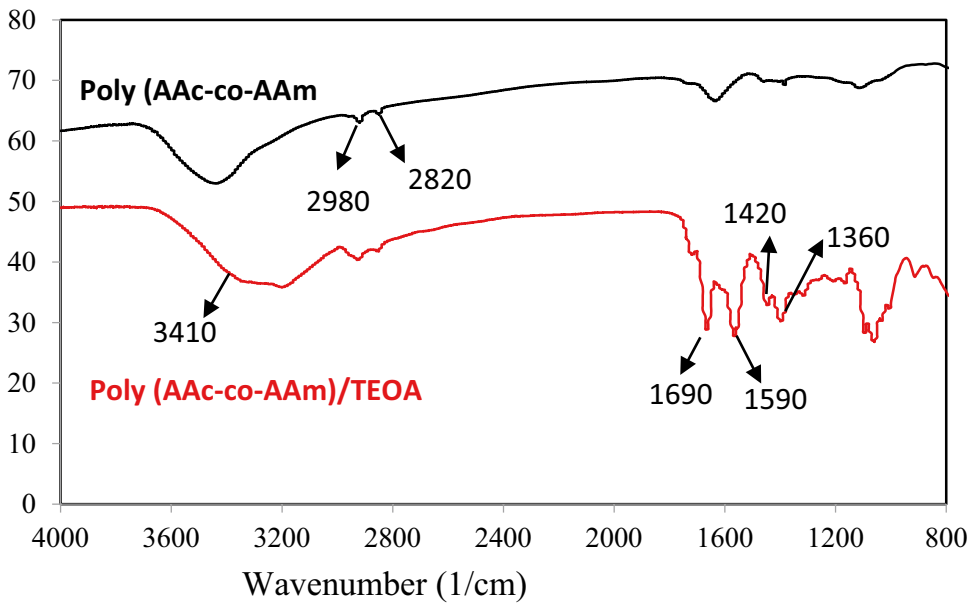

Fig. 1 FTIR spectra of Poly (AAc-co-AAm) and Poly (AAc-co-AAm)/TEOA

Table 3 The effect of aging time and COS content on the crosslink density of NBR composite

Crosslink density (g^{-1}.mol) × 10^{5}				
Aging time	0 day	1 day	3 days	7 days
COS 0	71.89	59.17	55.48	54.10
COS 2.5	63.53	67.64	68.72	71.55
COS 5	60.44	67.93	68.10	69.86
COS 7.5	59.22	67.30	69.20	72.80
COS 10	57.47	62.83	65.02	65.02

composite decreased from 71.89 *10^{-5} g^{-1}.mol for composite COS 0 to 63.5310 $^{-5}$ g^{-1}.mol after the addition of 2.5 phr of COS. The decrease in crosslink density continued to decrease with the increase in COS content within the NBR composite. In addition, NBR is unsaturated, and so, it is particularly susceptible to the degradation process when exposed to thermo-oxidative aging which leads to the breaking of polymer chains. The breaking of polymer chains occurs via free radical chain reactions that produce oxygen-containing groups such as carboxylic acids, ketones, aldehydes, and epoxides [13]. This degradation process deteriorates the physico-mechanical properties of the rubber composite. Chemical antioxidants are frequently added to diene elastomers to capture free radicals and slow down the ageing process. These anti-oxidants can greatly increase rubber's thermo-oxidative stability [26, 27]. The small antiaging compounds can be lost through diffusion to the surface of the composite, followed by evaporation. For a soluble antioxidant, it may be dissolved in appropriate solvent when the composite comes into contact with it [28]. To avoid the loss of antiaging molecules, macromolecular or polymeric antiaging molecules were used [19]. Many acrylamide based polymeric antiaging compounds were used to improve the aging properties of different polymers [29, 30]. The antiaging efficiency can be evaluated via retention in the mechanical properties of the composite containing the antiaging compound [31]. Table 3 also showed the anti-thermal aging action of COS, where the crosslink density within COS 0 composite decreased dramatically with the increase in aging time, whereas the COS containing composites displayed a good resistance to thermal aging as indicated from the increase of crosslink density with the increase in aging time. The crosslink density dropped from 71.89*10^{-5} g^{-1}.mol for COS 0 to 54.10 *10^{-5} g^{-1}.mol with retention value of -24.74% after aging at 70 °C for 7 days as indicated from. The COS 7.5 gave the highest crosslink density value of 72.80 *10^{-5} g^{-1}.mol with retention value of 22.93%. The retention in crosslink density value increases with the increase in COS content up to 7.5 phr then decreased where it recorded a retention value of 13.14% for COS 10 after 7 days of aging as indicated in Fig. 2.

Tensile properties

The tensile properties of NBR composites including different COS contents are represented in Fig. 3. It can be seen that, the tensile strength of NBR composite decreased gradually with the increase of COS content. The tensile strength decreased by 11.1% after addition of 2.5 phr of COS and reached to 18.8% after the addition of 10 phr, compared to COS 0. The decrease in tensile strength may be attributed the decrease in crosslink density with increasing COS within the composite. The direct effect of crosslink density within a polymeric composite on its mechanical properties has been extensively discussed in previous literature, where mechanical properties such as tensile strength, elastic modulus, and hardness properties increase while elongation at break decreases with increasing crosslink density [32–35]. Similar results were obtained here, where tensile strength decreased as crosslink density of NBR composite

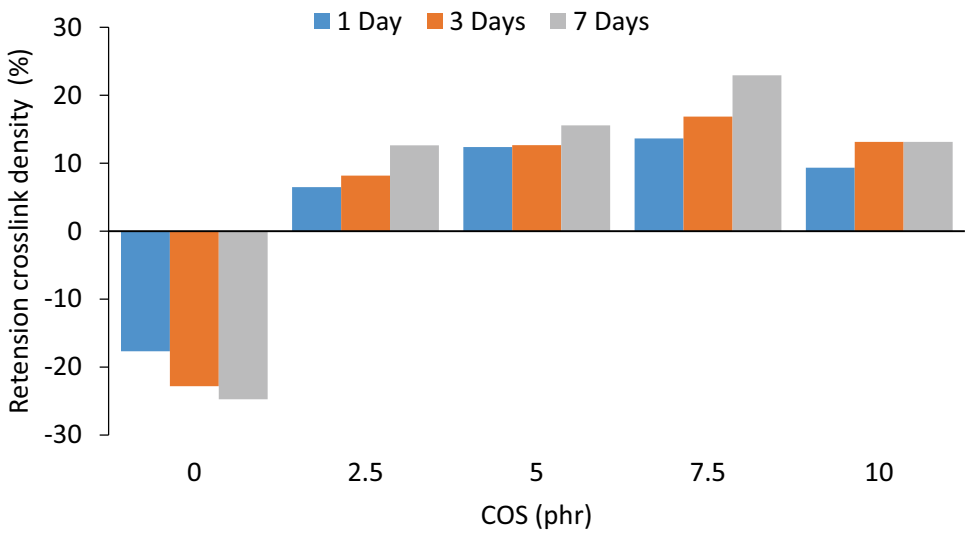

Fig. 2 Effect of COS content and aging time on the crosslink density value of NBR composite

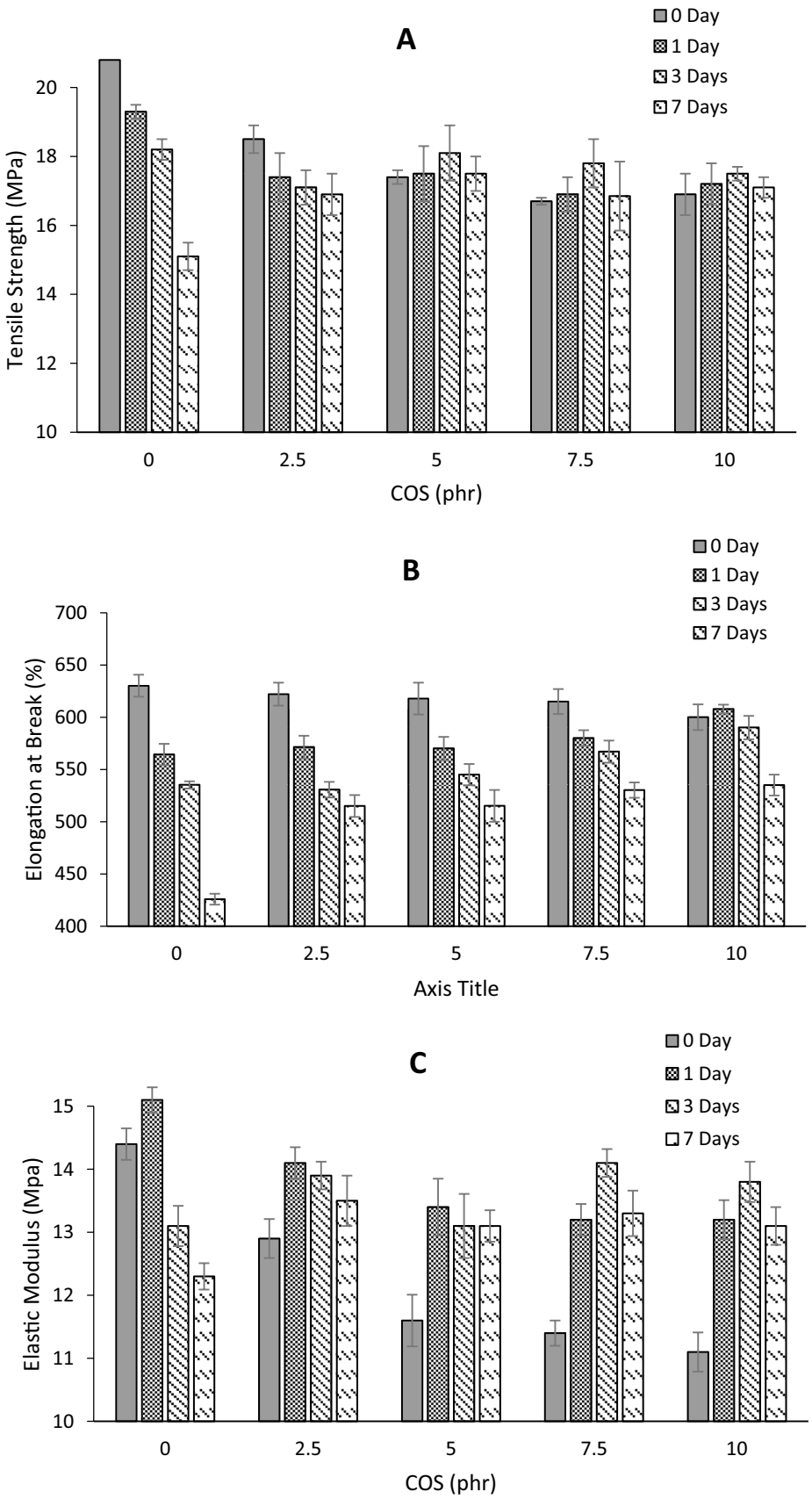

Fig. 3 Effect of COS and thermal aging on the: **A** Tensile strength; **B** Elongation at break; **C** Elastic modulus of NBR composite

Scheme 1 Preparation of triethanolamine salt of acrylamide/acrylic acid (COS)

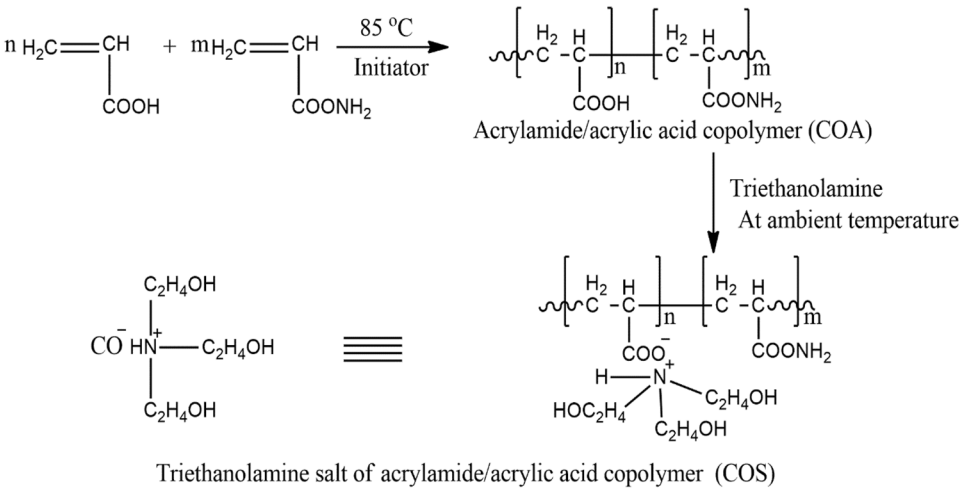

decreased. An accelerated thermo-oxidative aging test was carried out to evaluate the thermo-oxidative aging resistance of NBR composites with and without COS. In addition, with the increase of aging time the crosslink density within COS 0 decreased as a result of thermal degradation, and consequently, the tensile strength of COS 0 decreased sharply with the extension of aging time. The thermal oxidative aging resistance of COS may be due to the ability of amide and hydroxyl groups to supply its proton to react with the oxygen and hydrocarbon radicals and consequently delay the thermal degradation of NBR composite [36, 37]. It can be clearly seen that, the retention values of tensile strength for COS 0 were -7.2, -12.5 and -27.4 after exposure to aging for 1, 3 and 7 days, respectively, as indicated in Fig. 3A. The NBR composites containing COS exhibited more resistance to aging process. In addition, the retention value in tensile strength increased with increasing the COS content in the NBR composite, where the retention values in tensile strength of COS 2.5, COS 5, COS 7.5 and COS 10 after 7 days of aging were -8.6%, -1.7%, 0.6% and 1.2%, respectively. After 7 days of accelerated aging, the values of tensile strength of NBR containing composites were higher than that of COS 0, where the tensile strength values were 15.1, 16.9, 17.1,16.8 and 17.1 MPa for COS 0, COS 2.5, COS 5, COS 7.5 and COS 10, respectively. The effect of COS content and ageing time on NBR composite elongation at break is shown in Fig. 3B. It can be clearly seen, the elongation at break slightly decreased as the COS content increased within the NBR composite. Furthermore, the COS 0 composite showed a significant decrease in elongation at break value with increasing ageing time, with a decrease of 32.4% compared to the unaged COS 0 composite. The values of elongation at break after 7 days of aging for COS 0, COS 2.5, COS 5, COS 7.5 and COS 10 were 425.9,515.1, 515.2, 530.3 and 535.1% with retention values of -32.4, -17.2, -16.6, -13.8 and -10.8%, respectively. The elastic modulus increases as the rigidity and crosslink density within the composite increase [38, 39]. As indicated from Fig. 3C, the elastic modulus of COS 0 decreased as the aging time increased where the loss in elastic modulus of COS0 was 4.9, -9.0 and -14.6% after aging time of 1, 3 and 7 days. This could be attributed to the thermal degradation of polymer chains caused by thermal aging, which had a negative impact on crosslink density and thus on elastic modulus [33, 35]. The retention in elastic modulus for NBR composites containing COS as anti-aging agent was higher than that of COS 0 composite. The NBR composites which contain COS had a higher retention value in all tensile properties after aging and displayed higher tensile properties compared to COS 0 after aging for 7 days which confirms the high efficiency of COS as anti-thermal aging.

Adhesion mechanism

Scheme 1 shows the preparation of acrylamide/acrylic acid copolymer (COA), and its triethanolamin (TEA) salt (COS). The copolymerization was performed at temperature of 85 °C using the solution polymerization technique, followed by neutralization by triethanolamine at ambient temperature as indicated in Scheme 1. The Scheme 2 shows the preparation of the three dimensional resorcinol formaldehyde resin which is formed as a product of reaction between dry adhesion system components. The reaction began with the hydrothermal decomposition of hexamine to ammonia and formaldehyde. The liberated formaldehyde undergoes a condensation reaction with resorcinol molecules to give resorcinol formaldehyde resin (RF). The further condensation between RF molecules will form three dimensional RF resin (TRF) [40]. The synergist effect of dry adhesion system and COS on the adhesion between NBR and PET is indicated in Scheme 3. The hydroxyl groups of TEA attached to COS can condense with the hydroxyl groups of TRF compound

Scheme 2 Preparation of three dimensional resorcinol formaldehyde resin

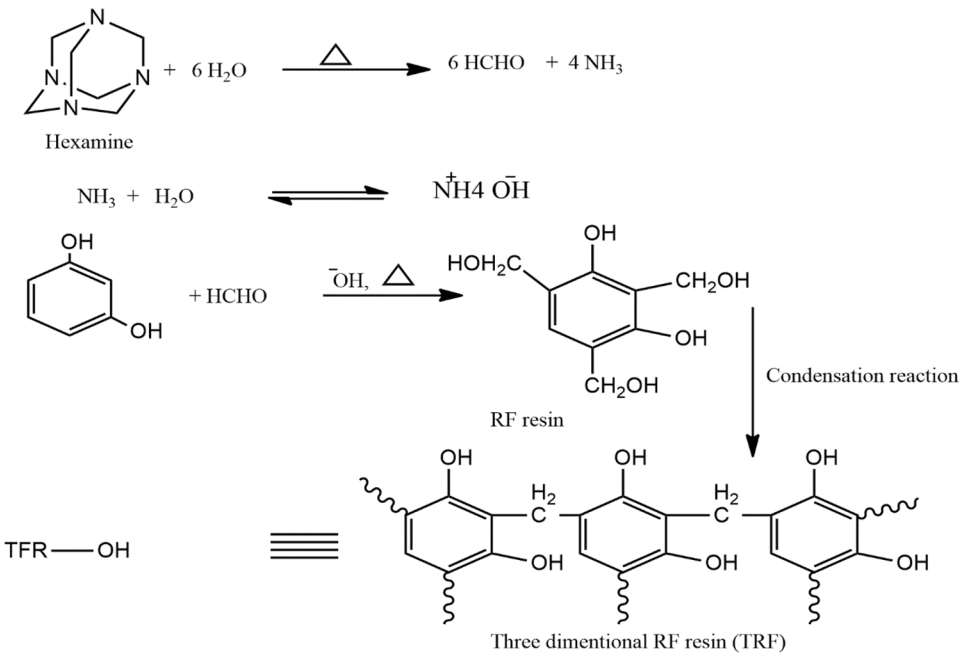

during vulcanization to form the TRF-COS adduct, which contains hydroxyl and amide groups. TRF-COS molecules bind to NBR via hydroxyl groups (-OH) added to the nitrile groups of NBR and to polyester (PET) fabric via hydrogen bonding and ester formation between free carboxylic groups of PET and hydroxyl groups of TRF-COS [7].

Adhesion properties

The addition of the adhesion promoter to the rubber formulation resulting in an improvement in the interfacial adhesion between rubber and substrates such as fabric. One of the methods that can be used to measure the improvement in the interfacial adhesion between rubber and fabric is the peel test, which involves determining the amount of force needed to separate two layers of PET fabric bonded to a layer of rubber. The 180° peel test was used to evaluate the influence of adhesion promoter (COS) on the peel strength of NBR sandwiched between two layers of PET fabric [41]. Figure 4 represents the effect of the COS amount on the peel strength. It can be seen that, the peel strength increased with the increase in COS amount up to 5 phr, then decreased. For unaged samples, the optimum dose of COS was 5 phr, which caused an improvement in peel strength of 16.4% in comparison with that of the COS 0 sample. TRF-COS molecules are rich in hydroxyl groups imparted by triethanolamine neutralization, which can interact with nitrile rubber through addition on the nitrile group and interact with PET

Scheme 3 Synergist effect of dry adhesion system and COS on the adhesion between NBR and PET

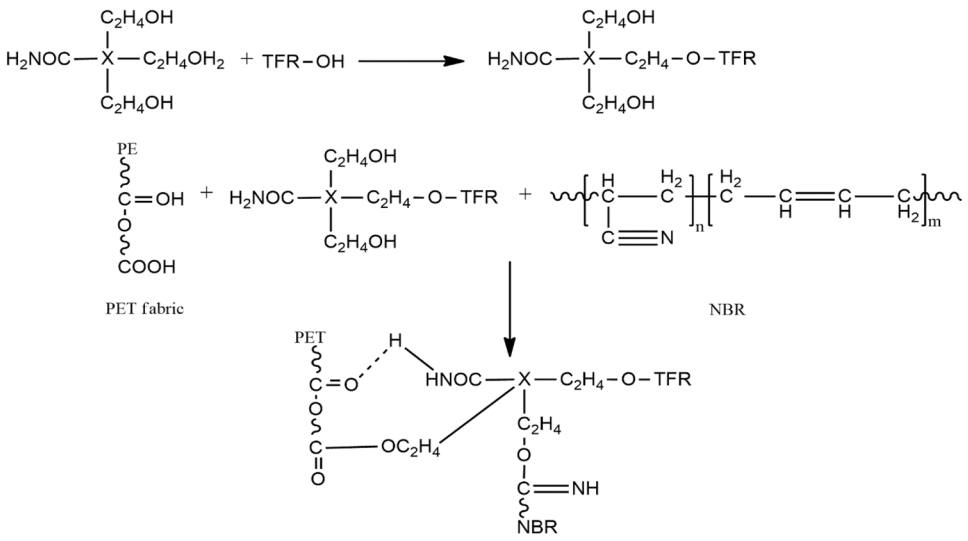

through hydrogen bonding and ester formation between free carboxylic groups of PET and hydroxyl groups of TRF-COS [7]. For aged samples, it can be clearly seen that the addition of COS improved the retention in peel strength with days of aging. The COS 0 sample showed a decrease in peel strength with time after exposure to heat for 7 days by 12.5% compared to the unaged sample. All samples that contain COS exhibited an increase in peel strength with increasing aging time (Days). The improvement in peel strength may be attributed to the reactions that assist the adhesion between PET and NBR, which may be activated by aging. Also It may be attributed to the crosslink cleavage in case of sample COS 0 increased with increasing the aging time, while the crosslink formation increased with the increasing the aging time for samples that contain COS as indicated in Table 3. The hydrogen atoms in COS can be liberated from the hydroxyl and amide groups and deactivate the peroxide radicals formed by ageing [36, 37]. The CO5 sample showed the highest peel strength within all intervals of aging, as indicated in Fig. 4.

Thermal properties

The thermal stability of different materials can be investigated using Thermogravimetric analysis (TGA). Also, TGA gives guidance on the temperature at which the material can be used without being subjected to thermal degradation. Figure 5A and B represents the TGA thermograms and their first derivative (DTGA) thermograms of NBR composites containing different COS contents. Table 4 shows the different thermogravimetric parameters such as the initial decomposition temperature (Ti), the temperature at which the rate of degradation becomes maximum (Tmax), the temperatures at which 30% (T30) and 60% (T60) weight loss take place, and the residue at 600 °C. It can be seen that from Fig. 5A and Table 4, the Ti value was shifted to a higher value after the addition of 5 and 10 phr of COS, where the Ti value of the NBR composite increased by 11.7 and 9.3 oC, respectively. This indicates that, the addition of COS to NBR composite shifted the service temperature to a higher value and delayed the thermo-oxidative degradation of NBR composite [42, 43]. In addition, the T30 and T60 increased with the increase of COS within the NBR composite. The residue at 600 °C wasn't significantly changed by addition of COS to NBR composite. Figure 5B depicts the thermal degradation of an NBR composite containing varying levels of COS in a single step. Also, the Tmax was shifted to a higher value with increasing COS content in the NBR composite where it increased by 16.2 and 26.3 °C, compared with that of COS 0, after addition of 5 and 10 phr of COS, respectively. The results obtained from thermal analysis displayed that the addition of COS improved the thermal stability of NBR composite and confirmed the anti-thermal aging effect of COS. In addition, the improvement of thermal stability of NBR composite containing COS at higher temperature can be attributed to the higher values of crosslink density of COS 5 and COS 10 at higher temperatures [38, 44].

Air permeability

Figure 6 shows the effect of different concentrations of COS on the air permeability through the NBR coated PET fabric. The air permeability of rubberized fabric without COS showed the highest air premeability (2.7 $m^3/m^2/min$) compared to the other rubberized fabrics that contain COS.

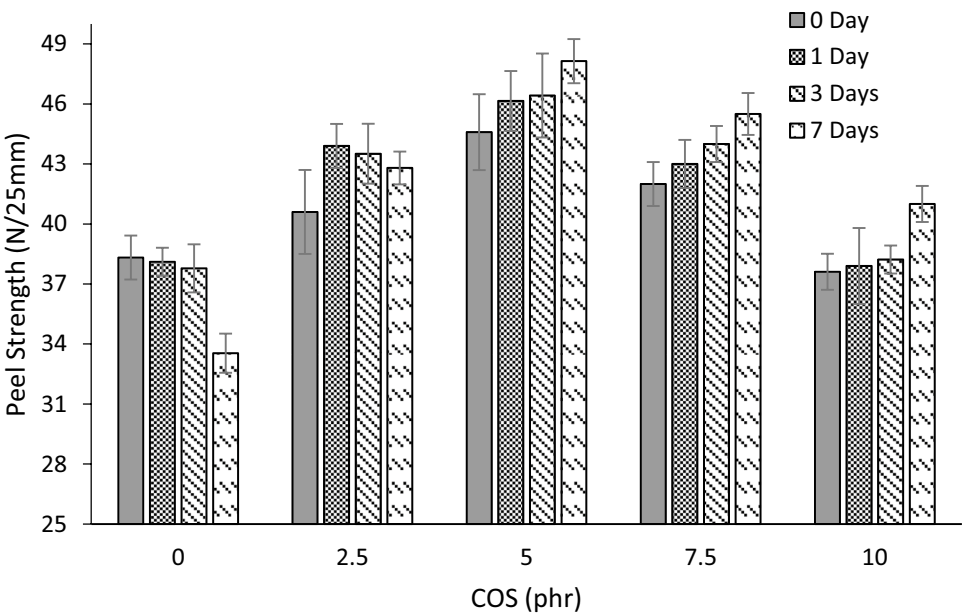

Fig. 4 Effect of COS and thermal aging on the adhesion between NBR and PET

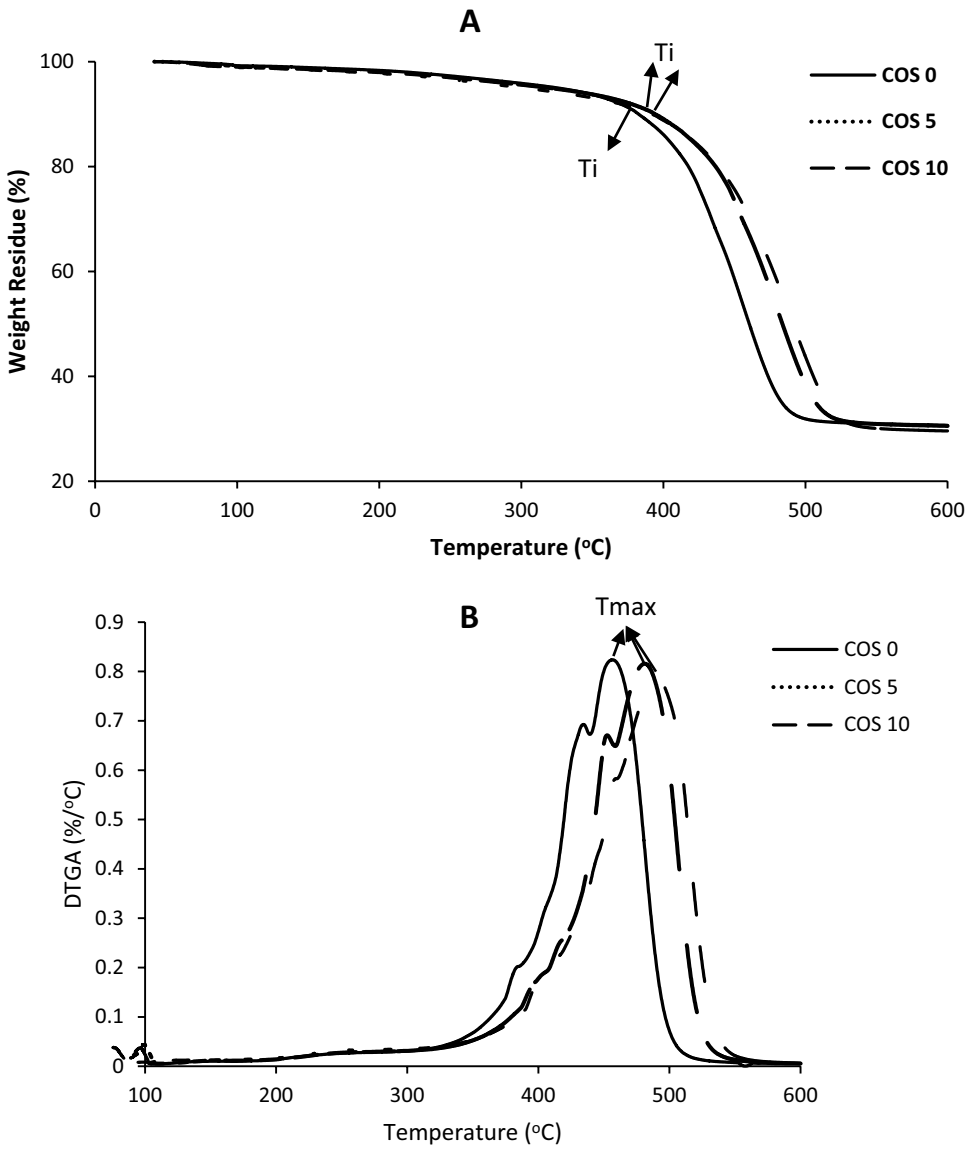

Fig. 5 The thermal properties of NBR composite containing different contents of COS: **A** TGA; **B** DTGA

he air permeability decreases dermatically as the COS concentration in the rubber mix increases. The air permeability decreased by 39.6% for COS 2.5 compared to that of COS 0, where it recorded 1.63 m^3/m^2/min. The air permeabilty continued to decrease with the increase of COS content within the rubber mix up to COS 7.5 then increased again with the increase of COS. The minimum values of the air permeability observed were 0.7 and 0.54 m^3/m^2/min recorded for COS 5 and COS 7.5, where the air permeability decreased by 74.1 and 80%, respectively. The decrease in air permeability of the coated fabric is related to the good adhesion between the different layers of rubber and fabric. The greater the adhesion between different fabric layers, the more compact the component and the greater its ability to slow the flow of gases within it. It is clear that the rubberized PET fabric containing COS has lower air permaeability and higher peel strength [45].

Table 4 The thermogravimetric parameters of NBR composite containing different contents of COS

Sample code	Ti	T30	T60	Tmax	Residue at 600 °C (%)
COS 0	382.5	433.9	473.6	460.1	30.3
COS 5	394.2	455.3	497.5	476.3	30.5
COS 10	391.8	460.3	505.4	486.4	29.5

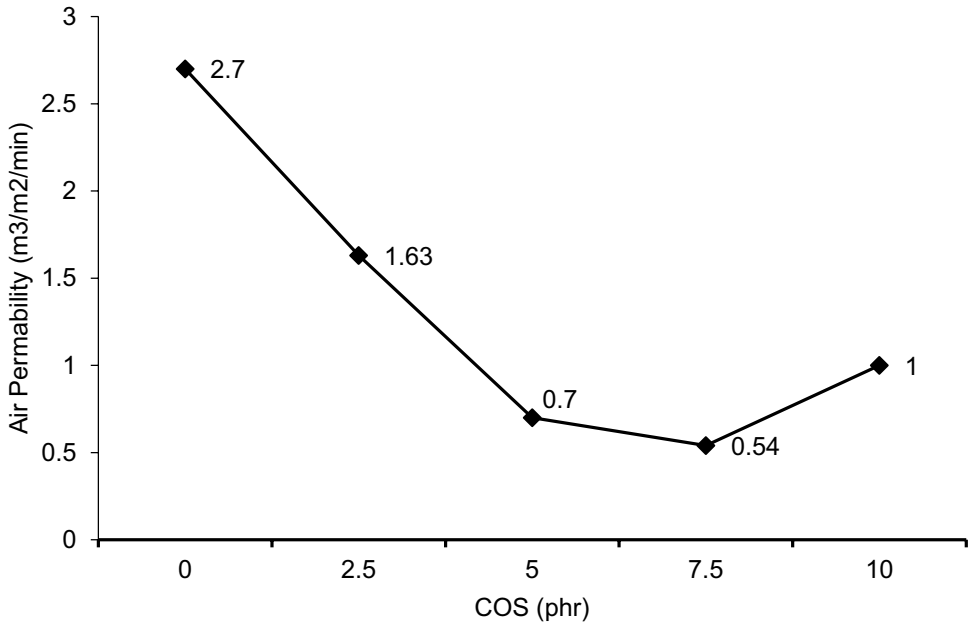

Fig. 6 The effect of COS on the air permeability of NBR/ PET sandwich

Conclusion

In this study, the structure of the prepared COS was confirmed using FTIR. The effect of different levels of COS on the mechanical properties, including the tensile properties of NBR composite and the adhesion between NBR composite and PET, was investigated. Furthermore, the thermal oxidative aging resistance of COS was evaluated. Tensile properties of NBR composites containing COS showed higher values after 7 days of ageing and a higher retention percentage than COS 0. The adhesion strength between NBR composite and PET improved by 16.4 % in comparison with that of COS 0 sample after addition of COS up to 5 phr to NBR composite. Almost all NBR composites containing COS showed an increase in tensile properties and peel strength as ageing time increased. The COS displayed good thermal oxidative aging resistance, whereas all NBR composites containing COS showed a good retention in all mechanical properties investigated after exposure to accelerated aging. The addition of COS improved the thermal stability of NBR composite where the Ti, T30, T60, and Tmax of NBR composite increased after the addition of COS. The improvement in thermal stability of NBR confirms the anti-aging properties of COS. The air permeability of the PET/NBR sandwich was improved in the presence of COS. Based on this study, the PET/NBR sandwich can be applied in many applications, such as: fuel pump diaphragms, belts, aircraft hoses, seals, gas tanks, and gaskets.

Funding Open access funding provided by The Science, Technology & Innovation Funding Authority (STDF) in cooperation with The Egyptian Knowledge Bank (EKB).

Data availability The data that support the findings of this study are available from the corresponding author, upon reasonable request.

Declarations

Conflicts of interest On behalf of all authors, the corresponding author states that there is no conflict of interest.

References

1. Lawandy S et al (1997) Adhesion properties of butyl rubber-coated polyester fabric. J Adhes Sci Technol 11(3):317–325
2. Razavizadeh M, Jamshidi M (2016) Adhesion of nitrile rubber (NBR) to polyethylene terephthalate (PET) fabric. Part 1: PET surface modification by methylenediphenyl di-isocyanate (MDI). Appl Surf Sci 360:429–435
3. Doganci E (2021) Improving adhesion between polyester cord and rubber by using glycidyl-POSS. J Appl Polym Sci 138(3):49681
4. Zhang Z et al (2001) Plasma surface modification of poly (m-aramide) fabric for adhesion improvement to fluorosilicone rubber. J Adhes Sci Technol 15(7):809–822
5. Subramanian V, Nando GB (1988) Adhesion of polyvinylalcohol cord and fabric to polychloroprene rubber in the presence of dry-bonding agents. J Adhes Sci Technol 2(1):35–41

6. Fu Q et al (2020) Study on the Synthesis of Castor Oil-Based Plasticizer and the Properties of Plasticized Nitrile Rubber. Polymers 12(11):2584
7. Jincheng W, Yuehui C, Zhaoqun D (2005) Research on the adhesive property of polyethylene terephthalate (PET) cord and nitrile-butadiene rubber (NBR) system. J Ind Text 35(2):157–172
8. Matsubara M et al (2021) Effect of Fiber Orientation on Nonlinear Damping and Internal Microdeformation in Short-Fiber-Reinforced Natural Rubber. Exp Tech 45(1):37–47
9. Sanchez-Solis A et al (2000) On the properties and processing of polyethylene terephthalate/styrene-butadiene rubber blend. Polym Eng Sci 40(5):1216–1225
10. Razavizadeh M, Jamshidi M (2016) Adhesion of nitrile rubber to UV-assisted surface chemical modified PET fabric, part II: Interfacial characterization of MDI grafted PET. Appl Surf Sci 379:114–123
11. Jamshidi M et al (2005) Study on cord/rubber interface at elevated temperatures by H-pull test method. Appl Surf Sci 249(1–4):208–215
12. Han R et al (2021) Effects of titanate on the bonding properties of silicone rubber and polyester fabric. Polym Compos 42(5):2370–2379
13. Nie J et al (2020) Antioxidant effects on curing/processing and thermo-oxidative aging of filled nitrile rubber. Mater Chem Phys 253:123403
14. Wang M et al (2019) Rheological and aging behaviors of liquid rubber modified asphalt binders. Constr Build Mater 227:116719
15. Wei H et al (2015) Antioxidation efficiency and reinforcement performance of precipitated-silica-based immobile antioxidants obtained by a sol method in natural rubber composites. RSC Adv 5(112):92344–92353
16. Abd El-Ghaffar M, El-Nashar D, Youssef E (2003) Maleic acid/phenylene diamine adducts as new antioxidant amide polymers for rubber (NR and SBR) vulcanizates. Polym Degrad Stab 82(1):47–57
17. Jovanović S et al (2016) Mechanical properties and thermal aging behaviour of polyisoprene/polybutadiene/styrene-butadiene rubber ternary blend reinforced with carbon black. Compos B Eng 98:126–133
18. Zhong R et al (2018) Improving thermo-oxidative stability of nitrile rubber composites by functional graphene oxide. Materials 11(6):921
19 Herdan J, Giurginca M (1993) Grafting antioxidants. V Phenols with mercaptoheterocyclic substituents as antioxidants for dienic rubbers. Polym Degrad Stab 41(2):157–162
20. Abdelkhalik A et al (2019) Effect of iron poly (acrylic acid-co-acrylamide) and melamine polyphosphate on the flammability properties of linear low-density polyethylene. J Therm Anal Calorim 138(2):1021–1031
21. Ni Y-H, Ge X-W, Zhang Z-C (2005) Preparation and characterization of ZnS/poly (acrylamide-co-acrylic acid) dendritical nanocomposites by γ-irradiation. Mater Sci Eng B 119(1):51–54
22. Nesrinne S, Djamel A (2017) Synthesis, characterization and rheological behavior of pH sensitive poly (acrylamide-co-acrylic acid) hydrogels. Arab J Chem 10(4):539–547
23. Urrego Yepes W et al (2019) Mechanical and rheometric properties of natural rubber composites filled with untreated and chemically treated leather wastes. J Compos Mater 53(11):1475–1487
24. Abdel-Hakim A et al (2021) Effect of fiber coating on the mechanical performance, water absorption and biodegradability of sisal fiber/natural rubber composite. Polym Int
25. Nakason C, Kaesaman A, Eardrod K (2005) Cure and mechanical properties of natural rubber-g-poly (methyl methacrylate)–cassava starch compounds. Mater Lett 59(29–30):4020–4025
26. Rashid A et al (2019) Fabrication, characterization and aging influence on characteristics of high temperature vulcanized silicone rubber/silica hybrid composites for high voltage insulation. Materials Research Express 6(10):105327
27. Lu Y et al (2008) Synthesis and aging properties of reactive antioxidant NAPM in natural rubber vulcanizates. J Appl Polym Sci 108(1):576–582
28. El-Wakil AEAA et al (2022) Enhancement of aging resistance of EPDM rubber by natural rubber-g-N (4-phenylenediamine) maleimide as a grafted antioxidant. J Vinyl Add Tech 28(2):367–378
29. El-Wakil A (2006) Synthesis, characterization, and evaluation of natural rubber-graft-N-(4-aminodiphenyl methane) acrylamide as an antioxidant. J Appl Polym Sci 101(2):843–849
30. Al-Ghonamy AI, Barakat MA (2010) Upgrading of acrylonitrile–butadiene copolymer properties using natural rubber–graft–N-(4-aminodiphenylether) acrylamide. J Appl Polym Sci 118(4):2202–2207
31. Wang H et al (2022) Mussel-inspired polydopamine functionalized silica as an effective antioxidant and reinforcer for elastomers. Compos Commun 29:101049
32. Abdel-Hakim A et al (2021) Effect of novel sucrose based polyfunctional monomer on physico-mechanical and electrical properties of irradiated EPDM. Radiat Phys Chem 109729
33. Abdel-Hakim A, El-Mogy SA, Abou-Kandil AI (2021) Novel modification of styrene butadiene rubber/acrylic rubber blends to improve mechanical, dynamic mechanical, and swelling behavior for oil sealing applications. Polym Polym Compos 09673911211031351
34. Ostad-Movahed S et al (2008) Comparing effects of silanized silica nanofiller on the crosslinking and mechanical properties of natural rubber and synthetic polyisoprene. J Appl Polym Sci 109(2):869–881
35. Saleh BK et al (2019) Effect of vinyltrimethoxysilane as a coupling agent on the mechanical and electrical properties of acrylic rubber. Egypt J Chem 62(5):921–936
36. Ding P et al (2022) Effects of a novel chitosan based macromolecule antioxidant COS-GMMP on the thermo-oxidative aging of styrene-butadiene rubber/silica composites. Polym Degrad Stab 195:109813
37. Luo K et al (2018) Effects of antioxidant functionalized silica on reinforcement and anti-aging for solution-polymerized styrene butadiene rubber: Experimental and molecular simulation study. Mater Des 154:312–325
38. Abdel-Hakim A, El-Mogy S, El-Zayat M (2019) Radiation crosslinking of acrylic rubber/styrene butadiene rubber blends containing polyfunctional monomers. Radiat Phys Chem 157:91–96
39. Abdel-Hakim A, Mourad RM (2020) Mechanical, water uptake properties, and biodegradability of polystyrene-coated sisal fiber-reinforced high-density polyethylene. Polym Compos 41(4):1435–1446
40. Liu D et al (2011) Simple hydrothermal synthesis of ordered mesoporous carbons from resorcinol and hexamine. Carbon 49(6):2113–2119
41. Krishna Prasad G et al (2017) Surface modification of nylon fabric and its optimization for improved adhesion in rubber composites. J Text Inst 108(6):1001–1009
42. Zou Y et al (2016) Antioxidative behavior of a novel samarium complex in styrene-butadiene rubber/silica composites. Polym Degrad Stab 133:201–210
43. Luo K et al (2019) Synergistic effects of antioxidant and silica on enhancing thermo-oxidative resistance of natural rubber: Insights from experiments and molecular simulations. Mater Des 181:107944
44. Abou-Laila M et al (2022) Gamma irradiation effects on styrene butadiene rubber/Pb3O4: Mechanical, thermal, electrical investigations and shielding parameter measurements. Radiat Phys Chem 192:109897

45. Shumkarova SP, Rajapova MN (2021) Influence of a mixture of different fibers on physical and mechanical properties of internal knitted fabrics. Sci Educ 2(4):271–274